COMMENT ON: LEHRMANN, D. J., BENTZ, J.M., WOOD, T., GOERS, A., DHILLON, R., AKIN, S., LI, X., PAYNE, J.L., KELLEY, B.M., MEYER, K.M., SCHAAL, E.K., SUAREZ, M.B., YU, M., QIN, Y., LI, R., MINZONI, M., HENDERSON, C.M., 2015, ENVIRONMENTAL CONTROLS ON THE GENESIS OF MARINE MICROBIALITES AND DISSOLUTION SURFACE ASSOCIATED WITH THE END-PERMIAN MASS EXTINCTION: NEW SECTIONS AND OBSERVATIONS FROM THE NANPANJIANG BASIN, SOUTH CHINA. PALAIOS, V. 30, P. 529-552.

STEVE KERSHAW[1], PIERRE-YVES COLLIN[2], SYLVIE CRASQUIN[3]

[1]*Department of Life Sciences, Brunel University, Uxbridge, UB8 3PH, UK;* [2]*Université de Bourgogne, CNRS UMR 6282 Biogéosciences, 6 Bd Gabriel, 21000 Dijon, France;* [3]*CR2P, MNHN-CNRS-UPMC Paris 6 – Sorbonne Universités, 4 place Jussieu, case 104, 75005, Paris, France*

e-mail: Stephen.kershaw@brunel.ac.uk

INTRODUCTION

In the study of Earth-surface environmental processes during the events associated with the Permian-Triassic boundary, a key issue is the nature of the latest Permian pre-extinction surface in shallow marine limestones in numerous sites, principally within the Tethyan realm. Sediments below this surface pre-date the extinction event, so that the limestones comprising these latest Permian facies contain diverse fossil remains of organisms that lived just before the extinction. At all reported sites, this surface is disconformably overlain by post-extinction sediments, which contain microbialites in many places, particularly in Tethys. The nature of the youngest pre-extinction surface remains controversial, originating by either physical erosion or dissolution. Furthermore, if the surface was created by dissolution, this could reflect ocean acidification or, alternatively, subaerial dissolution. These arguments were discussed by Collin et al. (2009) and Kershaw et al. (2012a).

In an attempt to solve the problem of the origin of the youngest pre-extinction surface, Lehrmann et al. (2015) provided a comprehensive treatment of the associated facies in the Nanpanjiang Basin in southern China, which although is of considerable value, contains some aspects we consider require further attention. Our comment primarily addresses their views regarding the environment of formation of calcium carbonate grain-coating cements in the boundary facies. We also consider some other aspects of their paper, all presented under several subheadings on specific points listed below. Thus, in this comment, we aim to clarify some of their reported observations and interpretations of the boundary facies.

In preparing this comment, we reviewed thin sections used by Collin et al. (2009) and present further photographs showing the fabrics in better detail. Figure 1 shows outcrop views of a key site in the Great Bank of Guizhou (for location see Lehrmann et al., 2015, their Fig. 1). Figure 1C is a polished block showing there are two truncation surfaces in the latest pre-extinction facies, close together just below the post-extinction microbialite. Figure 2 shows the lower truncation surface and eroded clasts from the underlying sediment incorporated into the sediment above the surface.

POINT 1: PENDENT CEMENTS

Lehrmann et al. (2015) assembled detailed measurements of thicknesses of isopachous cements encrusting the grains in the grainstone below the final pre-extinction surface to reveal that those cements vary in thickness but the variation does not have a uniform orientation. Specifically, according to Lehrmann et al. (2015), the thicker parts of the cements do not consistently point downwards and Lehrmann et al. (2015) used this information to “refute” (in their words) the interpretation of Collin et al. (2009) of the presence of pendent cements (which should of course all point downwards) and meniscus cements.

Lehrmann et al. (2015, caption for Fig. 12D) state there is a single generation of cement. Figures 3, 4, 5 and 6 of this comment, some of which are higher resolution versions of photographs published in Collin et al. (2009), show a thin rind of well-displayed isopachous fibrous cement formed at an early stage in the diagenetic history of the deposit. This rind did not cover all grains: some have prominent fibrous isopachous cement while others have little or none. Some grains have eroded/dissolved margins, and some of those have the early isopachous cement. A few grains show the first generation of fibrous isopachous cement overgrown by a ***second*** generation of grain-coating cement that has variable thickness and commonly has a diffuse appearance, not being as neatly fibrous as the earlier isopachous cement. It is this ***later cement*** that is pendent on some of the grains (Figs. 4 and 5).

Although it is certainly true that the number of grains with pendent and meniscus cement is limited, the limestone in which they occur is an eroded remnant, only a few cm thick, of foraminiferal grainstone directly below the final pre-extinction surface (Fig. 1C), also illustrated by Collin et al. (2009) and Kershaw et al. (2007). The portion in which pendent and meniscus cements occurs extends no more than 5 cm (and commonly less) below the final pre-extinction surface because there is an earlier erosion surface on finer-grained grainstone facies on which the foraminiferal grainstone was deposited (Fig. 2), described further below. Thus we contend that the description of pendent cements in the foraminiferal grainstone by Collin et al. (2009) remains valid, but accept that they may well be sparsely preserved, noting that only a few samples of the foraminiferal grainstone were collected by Collin et al. (2009).

POINT 2) GEOPETAL SEDIMENT AND SEQUENCE OF EVENTS

Geopetal sediment in these rocks was deposited after the isopachous cement and is present in photographs in Lehrmann et al. (2015, Fig. 12). Rather oddly, in thin sections illustrated by both Collin et al. (2009) and Lehrmann et al. (2015), some of this geopetal material (which is quite dark) lines floors and vertical walls of small cavities and it may represent oxidation in vadose cavities, mentioned as an expectation by Lehrmann et al. (2015).

Lehrmann et al. (2015), wrote: “The internal sediment consists of a darker micrite followed by a more diffuse micritic and peloidal material (Fig. 12A, C). The dark micrite adheres to particle walls and the peloidal sediment forms irregular convex-upward surfaces forming ‘gravity-defying’ fabrics (Fig. 12A, C). The gravity-defying fabrics suggest a microbial origin for the internal sediment. The peloidal internal sediments contain foraminifers and ostracods demonstrating a marine origin (Fig. 12B). The internal sediment resembles microbial micritic and peloidal material found in internal cavities within constructional frameworks in the overlying microbial biostrome (Lehrmann 1999). Notably, the internal sediment contains the foraminifer *Rectocornuspira kalhori* (Fig. 12B) demonstrating a basal Triassic, Griesbachian age.”

Although the internal sediment resembles microbial micrite, this does not necessarily mean that it ***is*** microbial micrite. Based on our observations (see new photograph of this fabric in Figure 7), we suggest the following post-depositional history of the grainstone: 1) Partial dissolution of some grains in a possible subaerial setting (see Collin et al., 2009, their Figs. 4E and 5B). 2) Early isopachous cement develops on many but not all grains when marine water fills pores (Figs. 4 and 7). 3) Pores are drained by sea-level fall and become air spaces resulting in formation of pendent and meniscus cements (Figs. 4 to 7). Dark geopetal sediment came in when the pores were either water or air filled, both options demonstrating there was open access to the partially-cemented grainstone from the surface for fine sediment to filter in. The presence of Griesbachian faunas in the lighter-coloured peloidal geopetal sediment described by Lehrmann et al. (2015) indicates that some pore space was left open when sea level rose to begin deposition of the microbialite that grew on the final pre-extinction surface. Note that in figure 7 the geopetal sediment lies directly on the isopachous cement, thus some sediment entered the grainstone before the pendent and meniscus cements grew (see also the thin dark infilling between isopachous and meniscus cement in the center of Fig. 6). Thus the geopetal cement entered in two phases, the first phase prior to pendent and meniscus cement and the second phase likely coinciding with early microbialite growth, matching Lehrmann et al.'s (2015) description of dark followed by peloidal sediment, quoted above. 4) Final pore-filling with blocky calcite (Figs. 4 to 7). In addition, the foraminiferal grainstone also contains syntaxial cements on crinoids (Fig. 5, lefthand edge), dissolution features on the margins of some foraminifera, and recrystallization of many of the foraminifera (photos in Collin et al., 2009). There is thus a rather complex micro-history in the thin remnant foraminiferal grainstone directly underlying the youngest pre-extinction surface. Although the exact sequence of diagenetic events is not fully determinable, the presence of meteoric cements demonstrates an episode of sea-level fall prior to the deposition of microbialite in marine waters. The observation of pendent and meniscus cements might be limited if the surface of the foraminiferal grainstone was eroded to different degrees in different areas before the microbialite grew on it.

POINT 3) EROSIONAL HISTORY

Lehrmann et al. (2015, page 544) stated: “Collin et al. (2009) interpreted two successive, stratigraphically distinct truncation surfaces beneath the microbialite at Langbai. We disagree with this interpretation; the upper of the two surfaces illustrated by Collin et al. (2009) is a stylolite (Collin et al. 2009, figs. 3c, 4b).”

We stand by our 2009 interpretation. Figures 3c and 4b of Collin et al. (2009) show the final pre-extinction surface. However, Kershaw et al. (2012a) presented highly detailed photographs of this surface to highlight the importance of stylolites in relation to determining events in the Permian-Triassic boundary sequence. Their evidence shows that most of the contact between the latest pre-extinction surface and the microbialite is stylolitized, and only small portions reveal the original sedimentary contact.

Furthermore, the statement by Lehrmann et al. (2015) quoted above does not acknowledge the observation made by Collin et al. (2009) that the foraminiferal grainstone, which is the latest pre-extinction deposit, disconformably overlies a finer-grained grainstone with a sharp contact between them. Although this sharp contact is everywhere stylolitized, Collin et al. (2009) documented rounded clasts of the lower grainstone entrapped within the foraminiferal grainstone, proving the former was eroded. Examples are shown in Fig. 3E of Collin et al. (2009), repeated in Fig. 3C of Kershaw et al. (2012a), and further illustrated in Figs. 1C and 2 of this comment. Although both surfaces are stylolitized, there is no doubt that both record truncation, the lower one very close to the final pre-extinction surface.

POINT 4) OCEAN-ACIDIFIED DISSOLUTION SURFACE?

Lehrmann et al. (2015, page 542) wrote: “Payne et al. (2007) interpreted the surface to be a submarine dissolution surface based on observations from South China, western Turkey, and southern Japan. Collin et al. (2009) and Kershaw et al. (2012b), in contrast, interpreted the truncation surface to be formed by subaerial karst diagenesis on the basis of observations from Langbai section of South China. In both cases there is no debate that the surface formed by chemical dissolution rather than physical abrasion.” The photos in Payne et al. (2007) are of insufficient quality to draw conclusions, but Collin et al. (2009) made clear that several alternative interpretations of the final pre-extinction surface are possible and that we did not believe there was a clear-cut answer. We see no evidence of any major chemical action at this surface (beautifully illustrated in Lehrmann et al., 2015), although some foraminiferal grains in the final pre-extinction grainstone seem to have suffered degradation consistent with dissolution, as mentioned above. Although none of our samples contain clasts eroded from the final pre-extinction surface, within the microbialite, Lehrmann et al. (2015, page 539) state they exist but are rare. Thus, we are left with the view that physical erosion, via either subaerial exposure or submarine processes, must have played a role in the formation of this surface.

To be clear, the theory of ocean acidification and seafloor dissolution at the Permian-Triassic boundary is a logical consequence of Siberian volcanism, but to date, we are not aware of any published physical evidence to substantiate it. A recent development on this topic is the use of boron isotopes to interpret pH changes through the Permian-Triassic boundary interval (Clarkson et al., 2015) to interpret an ocean acidification event slightly higher in the Early Triassic in the *isarcica* zone (next above the *parvus* zone, the lowest of the Triassic conodont biozones). However, Clarkson et al. (2015) specifically excluded acidification in Permian-Triassic boundary facies from the United Arab Emirates equivalent to those discussed in this comment.

POINT 5) ISOTOPES

Lehrmann et al. (2015, page 547) wrote: “Linear correlation between $\delta^{18}O$ and $\delta^{13}C$ values indicates a simple overprint from lithification and burial diagenesis (Fig. 14A–D). Neither $\delta^{18}O$ nor $\delta^{13}C$ values show a negative shift at the truncation surface that would be consistent with subaerial diagenesis (Fig. 14E–J).” However, given that there was a negative swing in both $\delta^{18}O$ and $\delta^{13}C$ across the Permian-Triassic boundary reflecting global ocean change (Sun et al., 2012), discriminating between local meteoric and global marine processes in these facies is problematic, because negative $\delta^{18}O$ and $\delta^{13}C$ are also indicative of meteoric processes. Therefore any argument based on O and C isotopes regarding marine versus freshwater origin of the cements remains an area for debate.

POINT 6) OXYGENATION OF THE MICROBIALITE

With regard to the argument presented by Lehrmann et al. (2015) that the microbialites grew in oxygenated conditions, we agree that the microbialites were probably oxygenated and that previous interpretations of low oxygen are probably incorrect (discussed by Collin et al., 2014; Kershaw, 2015).

REFERENCES

CLARKSON, M.O., KASEMANN, S.A., WOOD, R.A., LENTON, T.M., DAINES, S.J., RICHOZ, S., OHNEMUELLER, F., MEIXNER, A., POULTON, S.W., TIPPER, E.T., 2015, Ocean acidification and the Permo-Triassic mass extinction. Science, v. 348, issue 6231, p. 229-232.

COLLIN, P-Y., KERSHAW, S., CRASQUIN, S., FENG, Q., 2009, Facies changes and diagenetic processes across the Permian-Triassic boundary event horizon, Great Bank of Guizhou, South China: a controversy of erosion and dissolution. Sedimentology, v. 56, p. 677-693.

COLLIN, P.Y., KERSHAW, S., TRIBOVILLARD, N., FOREL, M.B., CRASQUIN, S., 2014, Geochemistry of post-extinction microbialites as a powerful tool to assess the oxygenation of shallow marine water in the immediate aftermath of the end- Permian mass extinction. International Journal of Earth Sciences. v. 104, p.1025-1037.

KERSHAW, S., 2015, Low verses high oxygenation of the seawater in which Permian-Triassic microbialites formed: Has the problem been solved? 31st IAS Meeting of Sedimentology, 22-25 June, 2015, Kraków, Poland, Abstracts, p. 268. www.ing.uj.edu.pl/ims2015

KERSHAW, S., LI, Y., CRASQUIN-SOLEAU, S., FENG, Q., MU, X., COLLIN, P-Y., REYNOLDS, GUO, L,. 2007, Earliest Triassic microbialites in the South China Block and other areas; controls on their growth and distribution. Facies, v. 53, p. 409-425.

KERSHAW, S., CRASQUIN, S., COLLIN, P-Y., LI, Y., FENG, Q. AND FOREL, M-B., 2009, Microbialites as disaster forms in anachronistic facies following the end- Permian mass extinction: a discussion. Australian Journal of Earth Sciences, v. 56, p. 809-813.

KERSHAW, S., CRASQUIN, S., LI, Y., COLLIN, PY., FOREL, M-B., 2012a, Ocean acidification and the end-Permian mass extinction: to what extent does evidence support hypothesis? Geosciences, v. 2, p. 221-234.

KERSHAW, S., CRASQUIN, S., LI, Y., COLLIN, PY., FOREL, M-B., MU, X., BAUD, A., WANG, Y., XIE, S., MAURER, F., GUO, L., 2012b, Microbialites and global environmental change across the Permian-Triassic boundary: a synthesis. Geobiology, v. 10, p. 25–47.

LEHRMANN, D.J., 1999, Early Triassic calcimicrobial mounds and biostromes of the Nanpanjiang basin, south China. Geology, v. 27, p. 359-362.

LEHRMANN, D. J., BENTZ, J.M., WOOD, T., GOERS, A., DHILLON, R., AKIN, S., LI, X., PAYNE, J.L., KELLEY, B.M., MEYER, K.M., SCHAAL, E.K., SUAREZ, M.B., YU, M., QIN, Y., LI, R., MINZONI, M., HENDERSON, C.M., 2015, Environmental controls on the genesis of marine microbialites and dissolution surface associated with the end-Permian mass extinction: new sections and observations from the Nanpanjiang Basin, South China. Palaios, v. 30, p. 529-552.

PAYNE, J.L., LEHRMANN, D.J., FOLLETT, D., SEIBEL, M., KUMP, L.R., RICCARDI, A., ALTINER, D. SANO, H., WEI, J., 2007, Erosional truncation of uppermost permian shallow marine carbonates and implications for Permian-Triassic boundary events. Geological Society of America Bulletin, v. 119, p. 771–784.

SUN, Y., JOACHIMSKI, M.M., WIGNALL, P.B., YAN, C., CHEN, Y., JIANG, H., WANG, L., LAI, X., 2012, Lethally hot temperatures during the Early Triassic greenhouse. Science, v. 338, p. 366–370.

FIGURE CAPTIONS

Figure 1. Field views (A and B) of the latest Permian pre-extinction facies at Rungbuo locality, Great Bank of Guizhou, southern China. See Lerhmann et al. (2009, Fig. 1) for location. In A, a key sample, R20, is illustrated. C) Polished vertical section showing that the post-extinction microbialite overgrew the irregular truncated surface of a coarse-grained foraminiferal grainstone, which itself overlies an eroded, finer-grained grainstone. See Figure 2 for details.

Figure 2. The contact between the two pre-extinction grainstones is a stylolite (A), but C shows one of a number of rounded clasts of the lower grainstone (B), demonstrating the lower contact was erosional.

Figure 3. Vertical thin section view of the topmost pre-extinction surface in sample R20 (Fig. 1) showing the irregular disconformity between the foraminiferal grainstone below and the post-extinction microbialite above (A). The blue box shows location of B, in which two prominent foraminiferal grains, lower center-right bear the pendent cements (arrowed) described by Collin et al. (2009); enlargements are given in Figures 4 and 5.

Figure 4. Enlargement of Figure 3, lower center-right, showing prominent fibrous isopachous rim cement on some grains, peloidal geopetal sediment in cavity floors, and a second generation of grain-coating cement on the isopachous cements on the two prominent foraminferal grains, center; the second generation cement is anisopachous, thickening downwards on the sides of the foraminifera. See Figure 5 for enlargement.

Figure 5. The two generations of grain-coating cement are well seen on the lower left-hand sides of the two foraminiferal grains illustrated here. The first cement

generation is fibrous isopachous rim cement, and the second generation is the anisopachous cement that has pendent features in this photograph and in Figure 4.

Figure 6. Another example of the two generations of grain-coating cements: a first prominent fibrous calcite and a second less obviously fibrous cement layer. The two cement generations are separated by a dark line, which is consistent with the dark geopetal sediment that was the first phase of pore-filling sediment, described in the text. In this example there is no evidence of pendent fabric but the second generation cement could be interpreted as meniscus cement.

Figure 7. A view of the upper grainstone in sample R20, a few mm below the final pre-extinction truncation surface (blue box in inset), showing thin geopetal dark material in cavities, deposited after the prominent fibrous isopachous cement. It is a matter of debate as to whether this sediment was deposited when the pore space was air-filled or water-filled, but both are possible.


A
B
C
10 20 30 40 50 60 mm

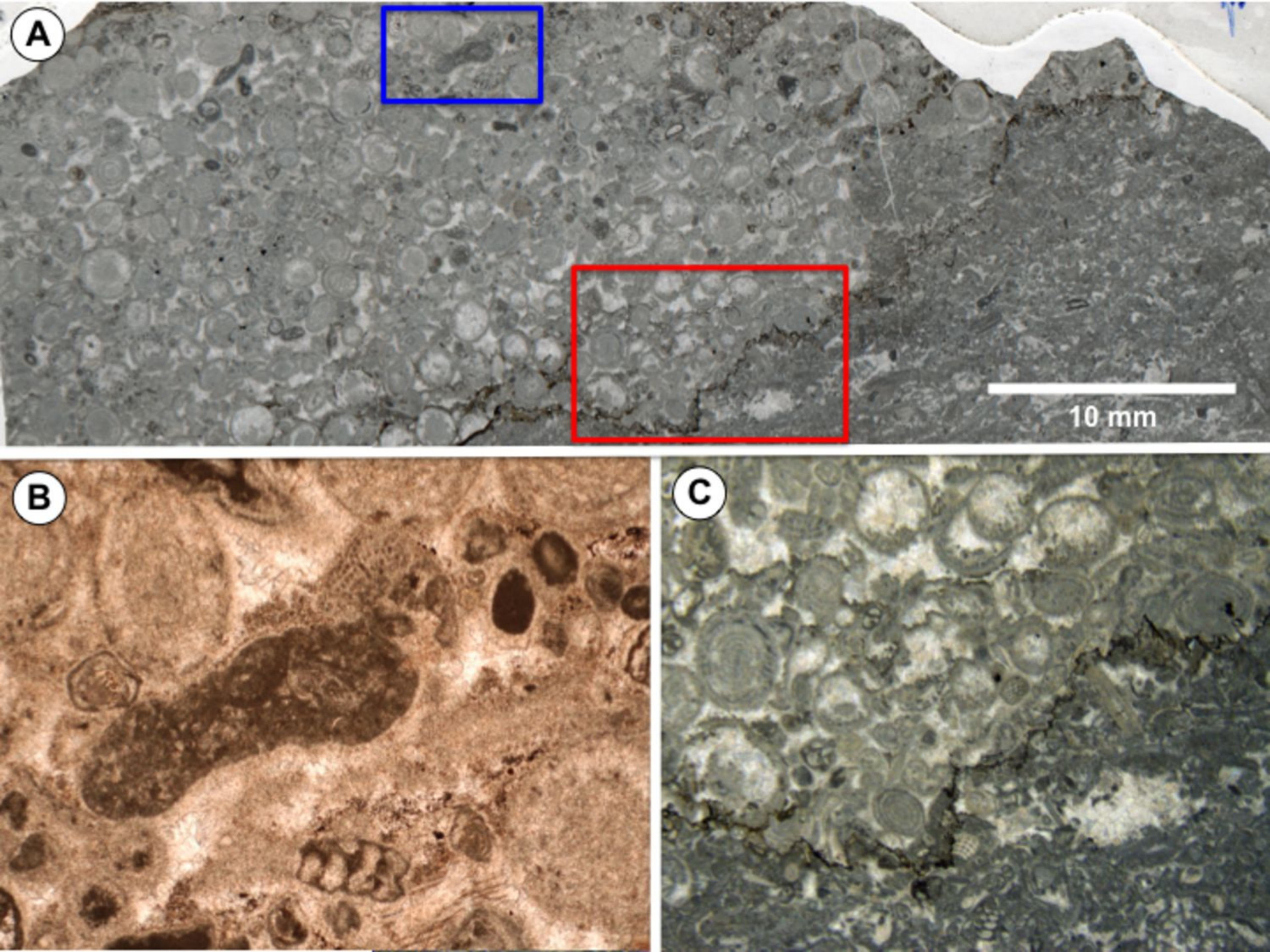
A
10 mm
B
C

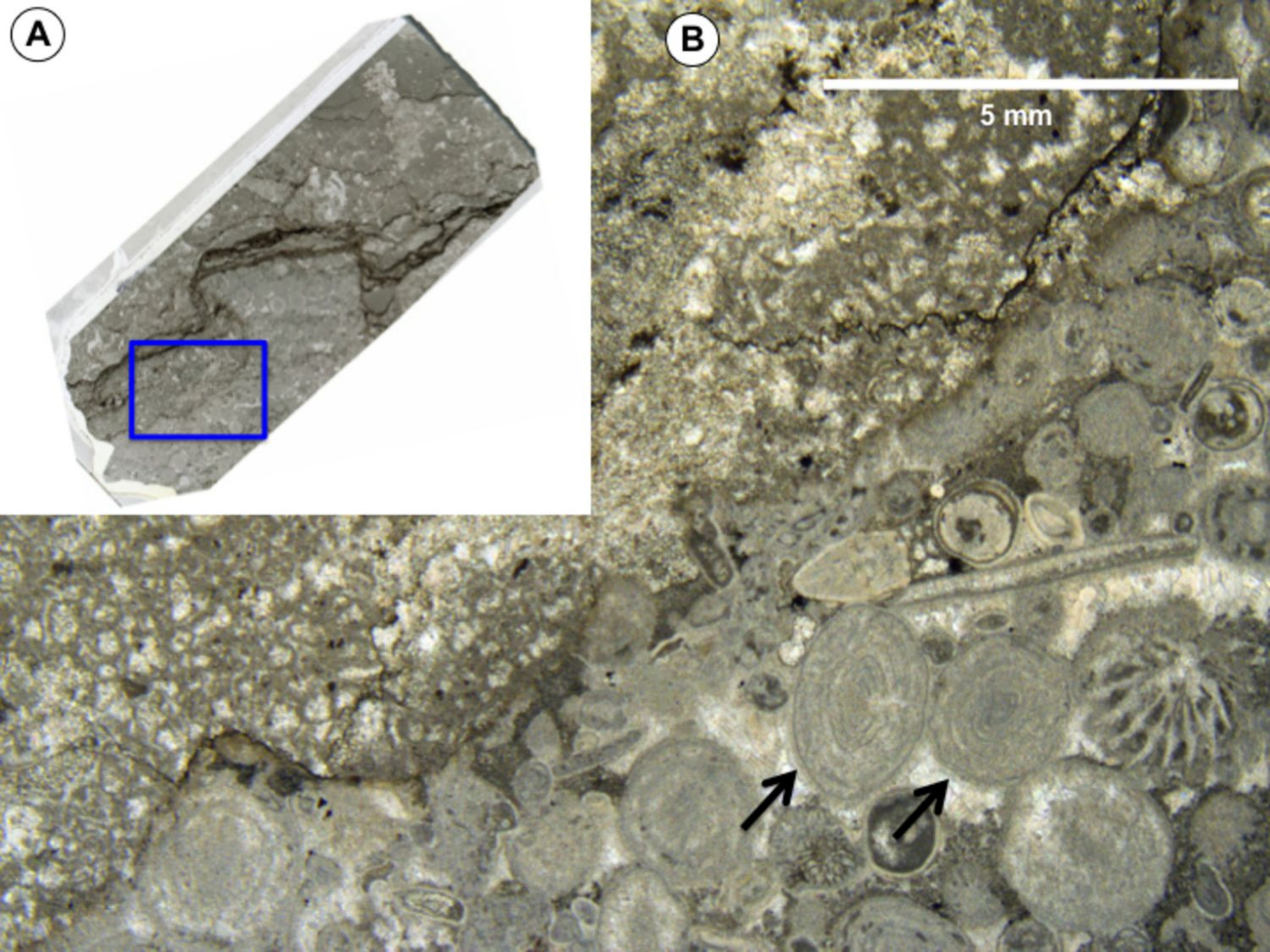
A
B
5 mm


2 mm

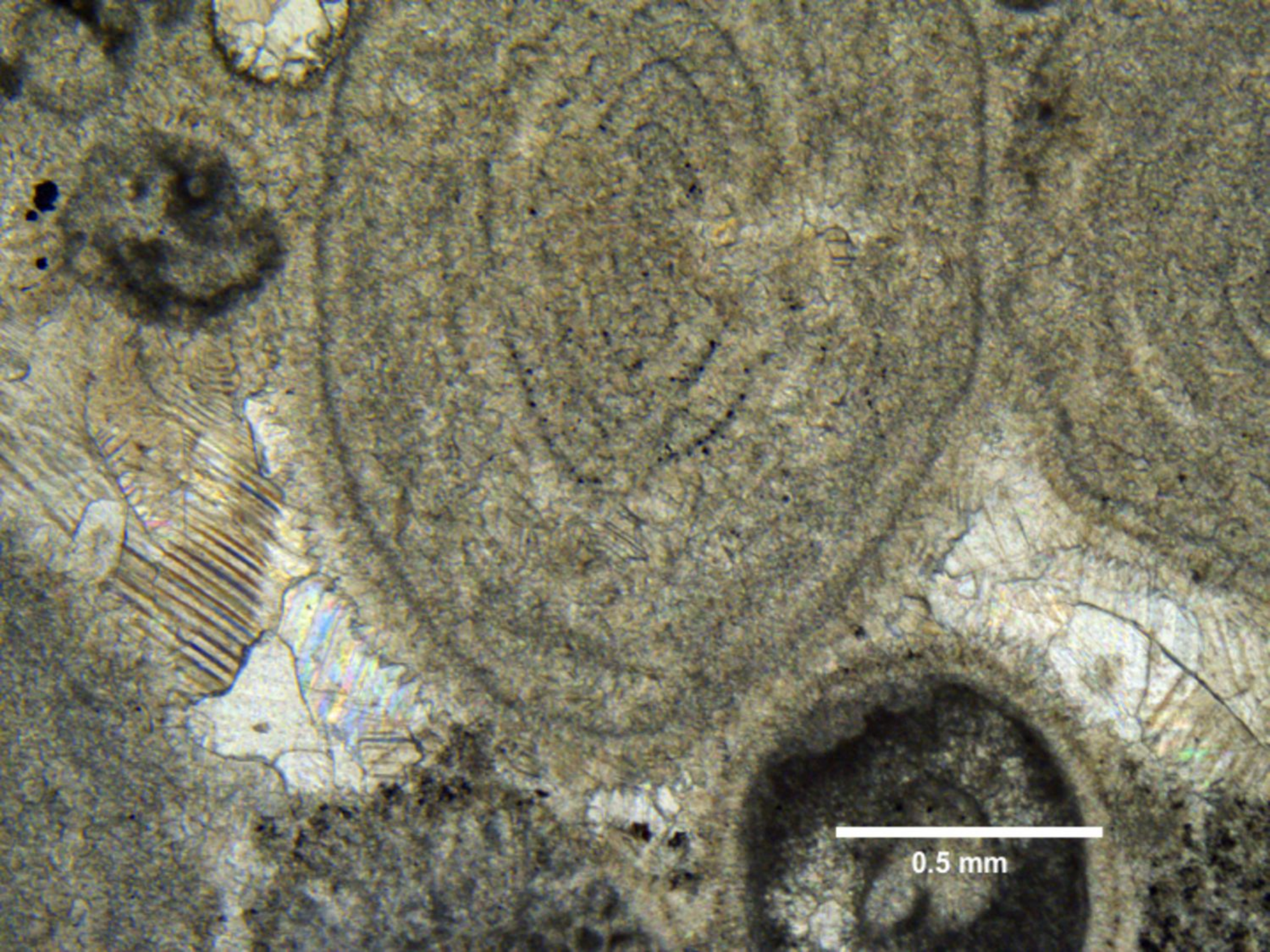
0.5 mm

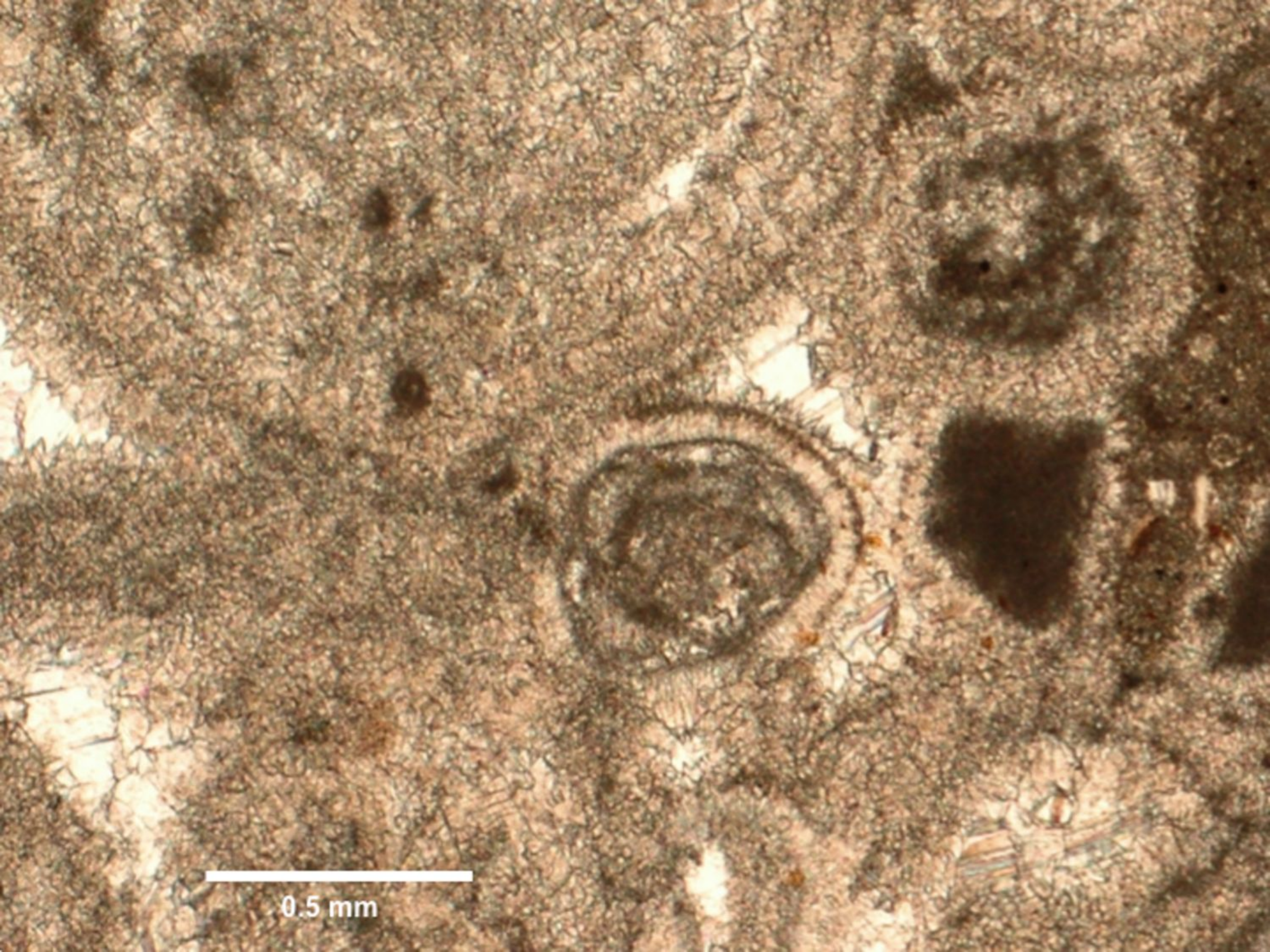
0.5 mm

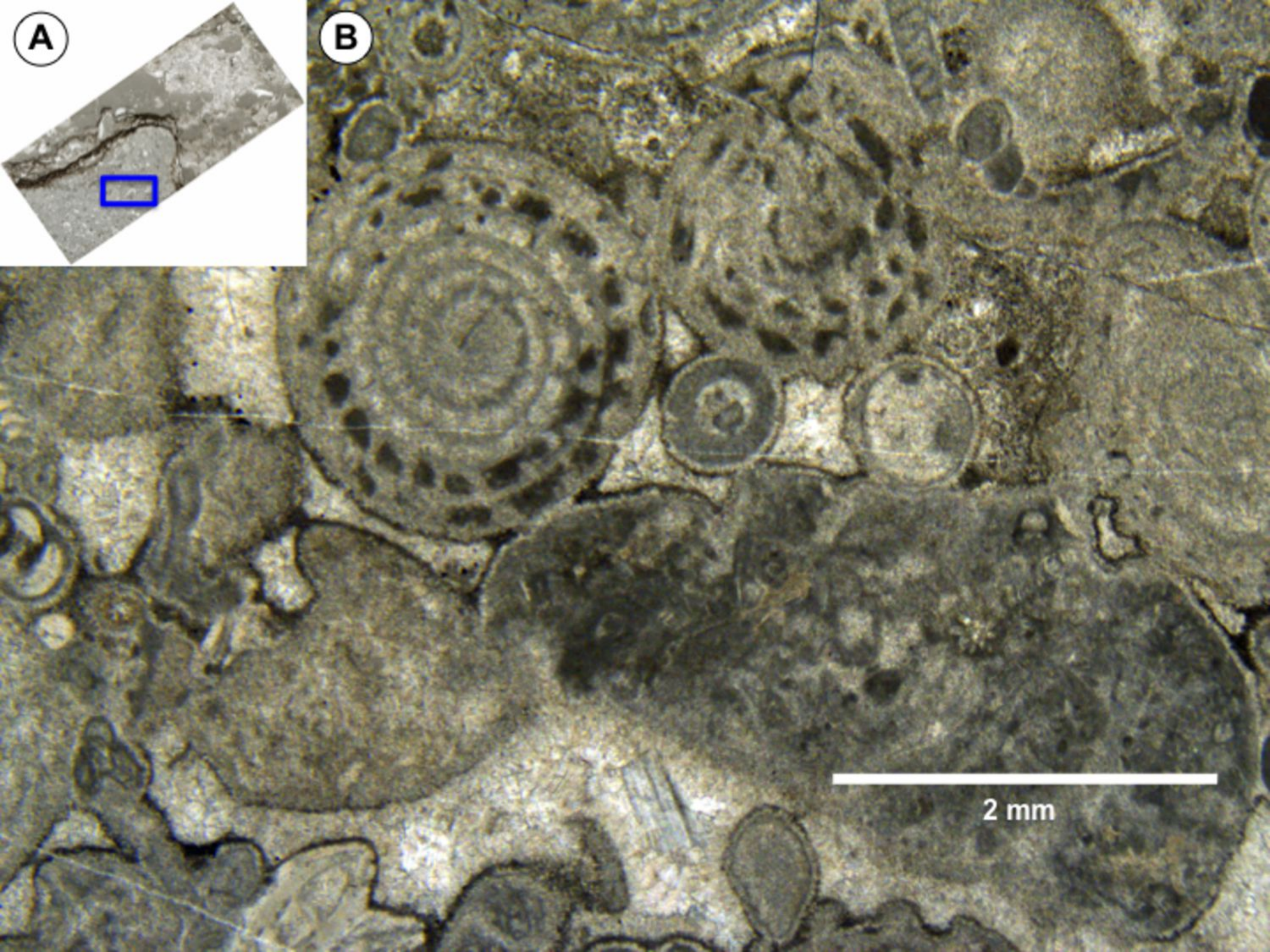
A
B
2 mm